

# Pressure effects on water vapour lines: beyond the Voigt profile

BY N. H. NGO<sup>1</sup>, H. TRAN<sup>1</sup>, R. R. GAMACHE<sup>2</sup> AND J. M. HARTMANN<sup>1,\*</sup>

<sup>1</sup>*Laboratoire Interuniversitaire des Systèmes Atmosphériques (LISA), CNRS (UMR 7583), Institut Pierre-Simon Laplace, Université Paris Diderot, Université Paris Est Créteil, 94010 Créteil Cedex, France*

<sup>2</sup>*Department of Environmental, Earth and Atmospheric Sciences, School of Marine Sciences, University of Massachusetts Lowell, 265 Riverside Street, Lowell, MA 01854-5045, USA*

A short overview of recent results on the effects of pressure (collisions) regarding the shape of isolated infrared lines of water vapour is presented. The first part of this study considers the basic collisional quantities, which are the pressure-broadening and -shifting coefficients, central parameters of the Lorentzian (and Voigt) profile and thus of any sophisticated line-shape model. Through comparisons of measured values with semi-classical calculations, the influences of the molecular states (both rotational and vibrational) involved and of the temperature are analysed. This shows the relatively unusual behaviour of H<sub>2</sub>O broadening, with evidence of a significant vibrational dependence and the fact that the broadening coefficient (in cm<sup>-1</sup> atm<sup>-1</sup>) of some lines increases with temperature. In the second part of this study, line shapes beyond the Voigt model are considered, thus now taking ‘velocity effects’ into account. These include both the influence of collisionally induced velocity changes that lead to the so-called Dicke narrowing and the influence of the dependence of collisional parameters on the speed of the radiating molecule. Experimental evidence of deviations from the Voigt shape is presented and analysed. The interest of classical molecular dynamics simulations, to model velocity changes, together with semi-classical calculations of the speed-dependent collisional parameters for line-shape predictions from ‘first principles’, are discussed.

**Keywords:** H<sub>2</sub>O; line shape; broadening; shifting; velocity effects

## 1. Introduction

Water vapour is a molecule of considerable importance for atmospheric physics through its active role in meteorology and climate; its distribution in the Earth atmosphere has been, for years, the focus of remote-sensing experiments. The latter are often based on recordings of absorption/emission spectra whose ‘inversion’ yields the atmospheric water vertical profile, and so accurate

\*Author for correspondence ([jean-michel.hartmann@lisa.u-pec.fr](mailto:jean-michel.hartmann@lisa.u-pec.fr)).

One contribution of 17 to a Theo Murphy Meeting Issue ‘Water in the gas phase’.

spectroscopic line parameters are obviously needed. This has motivated numerous experimental and theoretical laboratory studies in the past 50 years. Many consider the line positions (energy levels) and integrated intensities, which are intrinsic molecular parameters, independent of pressure and thus are not discussed in this study. If one considers densities at which the Doppler broadening is not fully dominant, then the line shapes can be described, to first order, by the widely used Voigt profile. Its parameters, which are the (Lorentz) collisional-broadening and -shifting parameters, have received considerable attention. Many measurements have been made from the microwave to the visible, providing data for thousands of transitions of pure H<sub>2</sub>O or in mixtures with various collisional partners [1,2]. Starting from the early Anderson–Tsao–Curnutte model [3,4], semi-classical approaches of increased complexity have provided better and better accuracy through the introduction of short-range forces [5,6] and a fully complex treatment [7]. Note that some of the problems associated with this approach have been recently discussed by Ma *et al.* [8]. The complex Robert Bonamy (CRB) semi-classical model is, today, the most reliable and tractable approach for the prediction of water-vapour-broadening and -shifting coefficients. As widely demonstrated (see earlier studies [9–11] and references therein), CRB calculations are accurate and enable, as discussed later, analyses of some unusual behaviours of the H<sub>2</sub>O line widths.

It is well known [12, ch. III] that even for collisionally isolated transitions unaffected by line mixing [12, ch. IV], the Voigt profile is approximate because it disregards two collisional effects. The first is the change of the radiating molecule velocity due to collisions, which leads, through the reduction of the Doppler width, to the so-called Dicke narrowing. The second is the dependence of the pressure-broadening and -shifting coefficients on the radiator (absolute) speed, which generally induces a narrowing and asymmetry of the lines. Such effects, pointed out for H<sub>2</sub>O transitions more than 20 years ago [13], have been the subject of numerous experimental and theoretical studies ([14–16] and references therein). A large variety of more or less sophisticated approaches have been proposed [12, ch. III] but, as discussed later, most of those applied to water vapour lines are crude and rely on the adjustment of ad hoc parameters on measured spectra.

The remainder of this study is divided into three sections. The first recalls some results obtained in the past decade from experiments and theory for the (usual) Lorentz-broadening and -shifting coefficients. The next section discusses non-Voigt effects and presents some very recent results obtained for pure H<sub>2</sub>O with a model that seems promising. Concluding remarks and directions for future studies are discussed in §4.

## 2. Lorentz-broadening (and -shifting) parameters

For most ‘usual’ molecules of atmospheric interest (CO, CO<sub>2</sub>, CH<sub>4</sub>, O<sub>3</sub>, O<sub>2</sub>, etc.), measurements (and calculations) demonstrate that the broadening coefficients  $\gamma$  by air have the following three characteristics [17]: (i) room temperature values show moderate variations with rotational quantum numbers and decrease by a factor of typically two from transitions involving low-to-high rotational energies ( $J$  values for a linear rotor), (ii) there is no evidence for any significant influence of the vibrational state, and (iii) the temperature dependence is accurately modelled

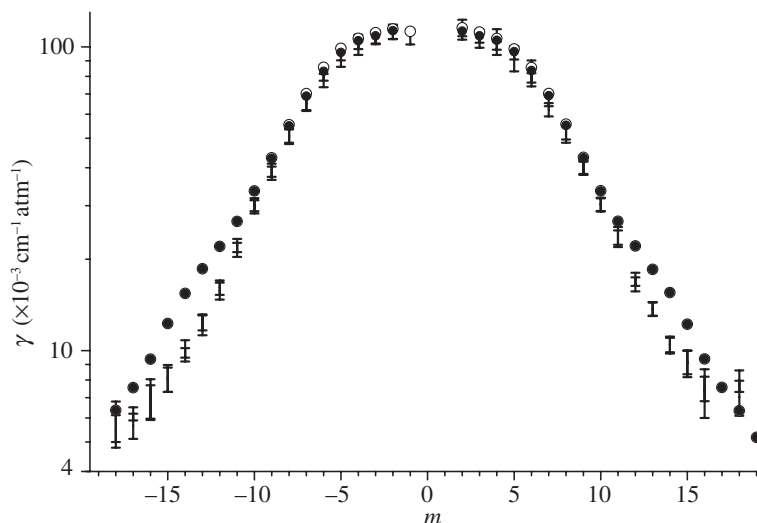


Figure 1.  $N_2$ -broadening coefficients for the  $K_c = J$  ( $J \pm 1_{1;J \pm 1} \leftarrow J_{0;J}$  and  $J \pm 1_{0;J \pm 1} \leftarrow J_{1;J}$ )  $P$  and  $R$  doublets of the  $\nu_2$  band. Symbols **I** are experimental values. Open circles and filled circles are calculated values associated with  $P$  and  $R$  lines such that  $(K_{a'} - K_{a''}) = (J' - J'')$  and  $(K_{a'} - K_{a''}) = -(J' - J'')$ , respectively. See Gamache & Hartmann [9] for details on the measured values and calculations.

though the widely used power law

$$\gamma(T) = \gamma(T_0) \left[ \frac{T_0}{T} \right]^n, \quad (2.1)$$

with  $n$  values typically between 0.6 and 0.8 (for  $\gamma$  in  $\text{cm}^{-1} \text{atm}^{-1}$ ). From these perspectives,  $H_2O$  lines show ‘unusual’ behaviours, similar to light rotors (e.g.  $HCl$ ,  $HF$ ) with largely spaced rotational levels. This fact is demonstrated by both experiments and semi-classical calculations.

- The broadening may strongly decrease with increasing rotational energies of the upper and lower states of the optical transition, and the decrease is greater when the rotational constant is high (i.e. large energies are reached for low  $J$  values). This is demonstrated in Gamache *et al.* [9], for instance, and shown in figure 1 for the lines with  $K_c = J$  ( $K_a = 0$  or  $1$ ). In this case, the quick increase with  $J$  of the energies involved in the collision-induced rotational jumps (i.e. changes of the rotational state) make collisions less and less efficient in broadening the line. As a result of this increasing non-resonance,  $\gamma$  varies by a factor of nearly 20 from  $J \approx 2$  to  $J \approx 18$ . This behaviour is quite well modelled ([9] and figure 1), with the CRB model using an unadjusted intermolecular potential. A better agreement between theory and experiments could be obtained by using an adjusted effective potential [10].
- Since high  $J$  lines with  $K_c = J$  show a very weak broadening owing to collision-induced rotational changes, they are favourable transitions for the detection of the influence of the vibrational dependence of the potential because, as analysed by Gamache *et al.* [9], this effect is masked for the

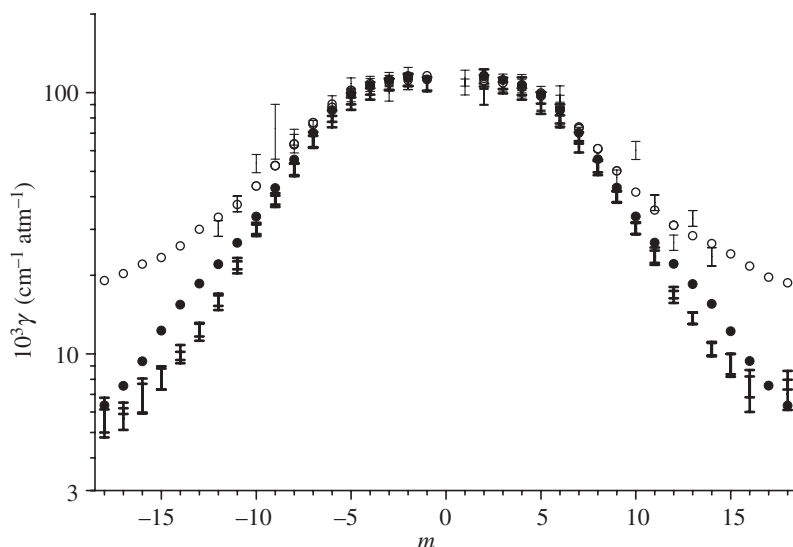


Figure 2.  $\text{N}_2$ -broadening coefficients for the  $K_c = J$  ( $J \pm 1_{1;J \pm 1} \leftarrow J_{0;J}$  and  $J \pm 1_{0;J \pm 1} \leftarrow J_{1;J}$ )  $P$  and  $R$  doublets. I (thin) and II (thick) are measured values, whereas open circles and filled circles are the corresponding calculated results for lines of bands involving a change of three quanta on stretching vibration or no change ( $\nu_2$  band). See Gamache & Hartmann [9] for details on the measured values and calculations.

broadest lines. In fact, experimental and theoretical values in figure 2 demonstrate that the broadening increases with vibrational difference between the upper and lower states.

- Finally, because the broadening of high  $J$  lines with  $K_c = J$  involves non-resonant large collision-induced rotational changes, one expects them to show unusual temperature dependencies. In fact, the increase of  $T$  makes their broadening easier, owing to the increase of the kinetic energy leading to a ‘resonance overtaking’ [18]. As a result,  $\gamma$  may increase with temperature so that the exponent  $n$  in equation (2.1) can be negative. This is confirmed by the measurements and calculations in figure 3. Starting from low  $J$  values for which  $n$  is close to the limit of five out of six, corresponding to purely resonant rotational jumps induced by the (dominant) dipole–quadrupole interaction,  $n$  decreases quickly with  $J$  (and becomes negative) as collisions become more and more non-resonant, and the relative contribution of close collisions increases.

The results presented earlier and in published studies [9–11] demonstrate that the CRB semi-classical approach provides reliable predictions of the pressure broadening (but also of the pressure shifting) of self- and  $\text{N}_2$ -broadened water vapour lines. Note that the Lorentz width at room temperature and the temperature dependence are accurately calculated. This is of importance for line-shape studies (§3) that require knowledge of the speed dependence of collisional parameters. Indeed, because the temperature dependence is accurately predicted

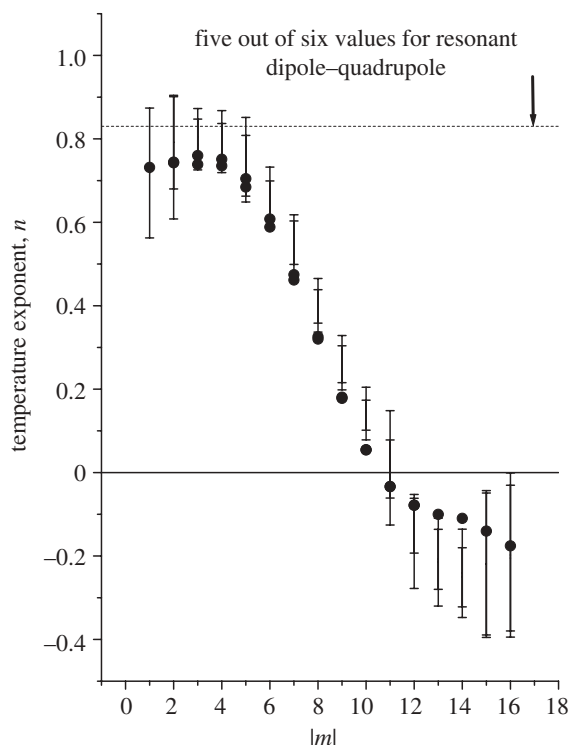


Figure 3. Temperature-dependent coefficient  $n$  (see equation (2.1)) for  $N_2$ -broadening coefficients of the  $K_c = J (J \pm 1_1; J_{\pm 1} \leftarrow J_{0;J}$  and  $J \pm 1_0; J_{\pm 1} \leftarrow J_{1;J}$ )  $P$  and  $R$  doublets of the  $\nu_2$  band. **I** are experimental values, whereas filled circles are the corresponding calculated results. See Wagner *et al.* [10] for details on the measured values and calculations.

(figure 3) and translates the effects of the (mean) relative speed, one expects that reliable values versus the absolute speed of the radiating molecule are predicted by CRB calculations.

### 3. The limits of the Voigt profile and ‘velocity effects’

As demonstrated for many molecular systems [12, ch. III] including  $H_2O$  ([14,15] and references therein), the Voigt (and Lorentz) profile is inappropriate. Except at very low pressures, for which the Gaussian Doppler shape is observed, fits of measured spectra with this line shape show residuals that—although small (a few %)—are now detected, owing to the high signal-to-noise ratio of modern laboratory and atmospheric measurements. When the absorption coefficient is adjusted, the associated measured – calculated differences (residuals) show a W-shaped signature characteristic of a narrowing (figure 4). This is due to the neglect of the changes of the radiator velocity induced by collisions and the dependencies of the collisional width and shift on the radiator speed.

Consider a collisionally isolated line (no line mixing) due to dipolar absorption and denote  $d(\mathbf{v}, t)$ , the autocorrelation of the dipole matrix element for the considered transition and the molecules having a velocity  $\mathbf{v}$ . The normalized

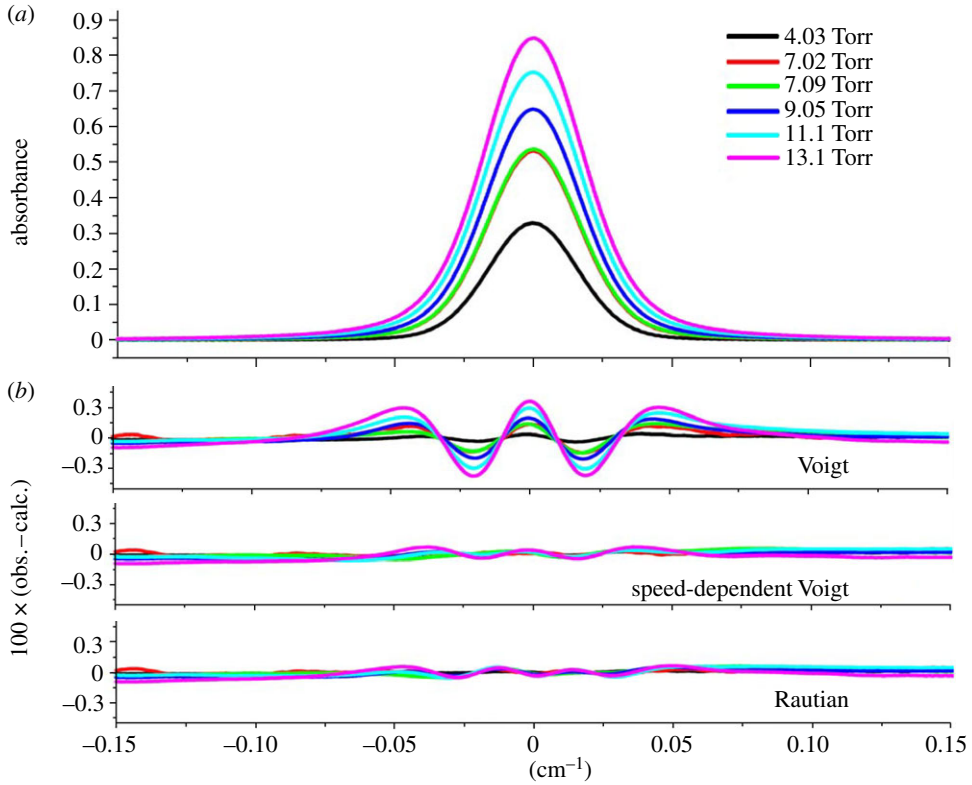


Figure 4. (a) Measured absorbance and (b) fit residuals obtained with the Voigt, speed-dependent Voigt and Rautian profiles for the  $6_{0,6} \leftarrow 5_{0,5}$  line of the  $2\nu_1 + \nu_2 + \nu_3$  band of pure  $\text{H}_2\text{O}$  at room temperature and various pressures. (Online version in colour.)

shape  $I(\omega)$  at angular frequency  $\omega$  ( $\omega = 2\pi c\sigma$ ,  $\sigma$  being the wavenumber) for a line of unperturbed position  $\omega_0$  is then obtained from the integration over all velocities and a Laplace transform, i.e.

$$I(\omega) = \frac{1}{\pi} \text{Re} \left\{ \int_0^{+\infty} e^{-i(\omega - \omega_0)t} \left[ \iiint d(\mathbf{v}, t) d^3\mathbf{v} \right] dt \right\}, \quad (3.1)$$

where  $\text{Re}\{\dots\}$  denotes the real part. If one assumes *no correlation* between the changes of the radiator velocity and of its internal state, then the time evolution of  $d(\mathbf{v}, t)$  is given by [12,19,20]

$$\begin{aligned} \frac{\partial}{\partial t} d(\mathbf{v}, t) = & - \left[ \iiint f(\mathbf{v}', \mathbf{v}) d^3\mathbf{v}' \right] d(\mathbf{v}, t) + \iiint f(\mathbf{v}, \mathbf{v}') d(\mathbf{v}', t) d^3\mathbf{v}' \\ & - [i\mathbf{k} \cdot \mathbf{v} + \Gamma_c(\mathbf{v}) - i\Delta_c(\mathbf{v})] d(\mathbf{v}, t), \end{aligned} \quad (3.2)$$

with

$$d(\mathbf{v}, t=0) = f_{\text{MB}}(\mathbf{v}) = (\tilde{\nu}^2 \pi)^{-3/2} \exp \left[ - \left( \frac{\|\mathbf{v}\|}{\tilde{\nu}} \right)^2 \right], \quad (3.3)$$

$f_{\text{MB}}(\mathbf{v})$  being the Maxwell–Boltzmann equilibrium distribution and  $\tilde{v} = \sqrt{2k_{\text{B}}T/m}$  the most probable speed. The first two terms in equation (3.2) take the effects of changes of the radiator velocity into account. The collision kernel  $f(\mathbf{v}, \mathbf{v}') d^3\mathbf{v} d^3\mathbf{v}'$  is thus the probability, per unit time, of a velocity change from  $\mathbf{v}'$  to  $\mathbf{v}$  (within small volumes  $d^3\mathbf{v}'$  and  $d^3\mathbf{v}$ ). The third contribution  $i\mathbf{k} \cdot \mathbf{v}$  ( $\mathbf{k}$  being the radiation wavevector) represents the dephasing due to the Doppler effect. Finally,  $\Gamma_c(\nu) - i\Delta_c(\nu)$  (proportional to the total pressure for a pure or highly diluted absorbing gas) monitors the damping and dephasing of  $d(\mathbf{v}, t)$  due to collision-induced internal relaxation ( $\Gamma_c(\nu)$  and  $\Delta_c(\nu)$  being the speed-dependent collisional width and shift of the optical transition).

Starting from equation (3.2), line shapes in limiting cases are obtained. For instance, disregarding velocity changes ( $f(\mathbf{v}, \mathbf{v}') = \delta_{\mathbf{v}, \mathbf{v}'}$  so that the first two terms cancel out) leads to the speed-dependent Voigt profile (SDVP). Further assuming no speed dependence and replacing  $\Gamma_c(\nu) - i\Delta_c(\nu)$  by its average over the Maxwell–Boltzmann distribution yield the Voigt profile. Similarly, purely Dicke-narrowed profiles are derived when the speed dependence is neglected, but velocity changes are taken into account. Within this frame, extreme cases correspond to soft (respectively, hard) collisions, which very slowly change the velocity (respectively, each collision completely thermalizes the velocity). These limit situations, occurring, respectively, for (very) large and small values of the radiator–perturber mass ratio, lead to the widely used Galatry [21] and Nelkin & Ghatak [22] (also called Rautian & Sobel'man [20]) profiles. As discussed in Hartmann *et al.* [12, ch. III], a great variety of combinations of such models has been proposed, with examples given for H<sub>2</sub>O in earlier studies [14,15]. To the best of our knowledge, except for Tran *et al.* [16], all analyses of non-Voigt profiles for H<sub>2</sub>O lines have been made using empirical models with parameters adjusted on measured spectra. For instance, up to six parameters monitor the correlated speed-dependent Nelkin–Ghatak profile used in Lisak *et al.* [14]. Such approaches have the advantage, provided that a sufficient number of parameters are fitted, of enabling agreement with measurements within less than 0.1 per cent and within the very small noise level of laser experiments ([14,15] and figure 4). Nevertheless, important problems remain. The first problem is that, in some cases illustrated in the bottom two panels of figure 4 (and figs 2, 4 and 6 of Lisak *et al.* [14]), two very different models may lead to similar agreements with measurements, thus preventing any reliable conclusion on the true mechanisms involved. The second, connected with the first, is that strong correlations between the adjusted parameters often occur, which limit the complexity of the model and which can be used unless some parameters are fixed to *a priori* values. Hence, except in some rare cases where one process is fully dominant, ambiguities generally remain, as confirmed by the following two figures. Figure 4, which displays pure H<sub>2</sub>O spectra for the  $6_{0,6} \leftarrow 5_{0,5}$  line of the  $2\nu_1 + \nu_2 + \nu_3$  band recently recorded [23] with the apparatus of Ibrahim *et al.* [24], shows the Rautian and SDV (using Rohart *et al.* [25]:  $\Gamma(\nu) = \Gamma_0 + \Gamma_2[(\nu/\tilde{\nu})^2 - 3/2]$ ) profiles both leading to very good fits, although these two models account for completely different processes. Furthermore, the adjusted parameters (figure 5) all show linear dependencies on pressure, so that no conclusion can be drawn on what really happens (likely a mixture of velocity changes and speed-dependent effects).

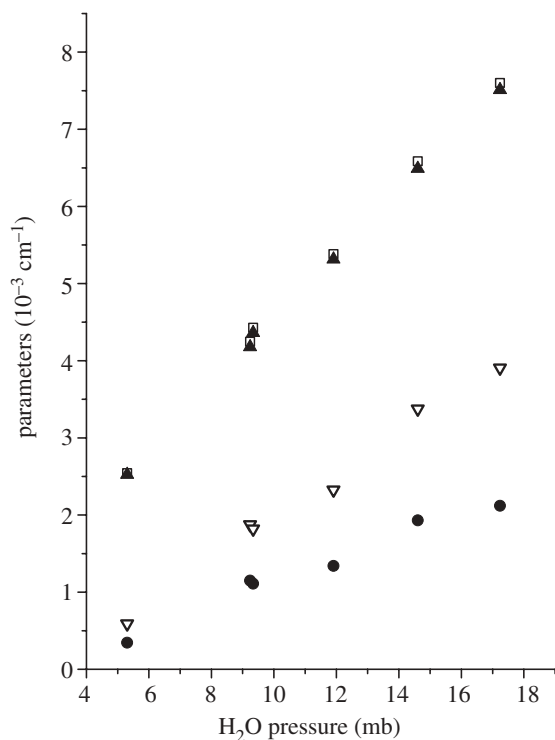


Figure 5. Pressure dependence of the parameters deduced from the fits of figure 4 with the speed-dependent Voigt profile (constant and quadratic components of the law  $\Gamma(v) = \Gamma_0 + \Gamma_2[(v/\tilde{v})^2 - 3/2]$ ) and the Rautian profile (broadening  $\Gamma$  and velocity changing frequency  $\nu_{VC}$ ). Squares, SDV  $\Gamma_0$ ; filled circles, SDV  $\Gamma_2 \times 5$ ; filled triangles, Rautian  $\Gamma$ ; open inverted triangles, Rautian  $\nu_{VC} \times 5$ .

In view of the problems inherent to the use of empirical models, we propose a different approach in which many parameters are fixed according to independent theoretical predictions. Indeed, using available accurate intermolecular potentials, one can calculate both velocity changes and the speed of collisional parameters as described in the following.

- Using the CRB approach of earlier studies [7,11], the broadening and shifting coefficients can be computed versus the relative (radiator–perturber) speed,  $v_r$ . The results in §2 and numerous papers by Gamache *et al.* make us confident in the accuracy of such predictions. From these, the dependencies on the absolute radiator speed  $v$  are straightforwardly obtained by Maxwell–Boltzmann averages over the perturber velocity  $\mathbf{v}_p$  through

$$X(v) = \frac{1}{\tilde{v}_p} \frac{2}{\sqrt{\pi}} \int_0^\infty dv_r X(v_r) \frac{v_r}{v} \operatorname{sh} \left[ \frac{2vv_r}{\tilde{v}_p} \right] \exp \left[ -\frac{v^2 + v_r^2}{\tilde{v}_p} \right], \quad (3.4)$$

$$X = \Gamma_c \quad \text{or} \quad X = \Delta_c,$$

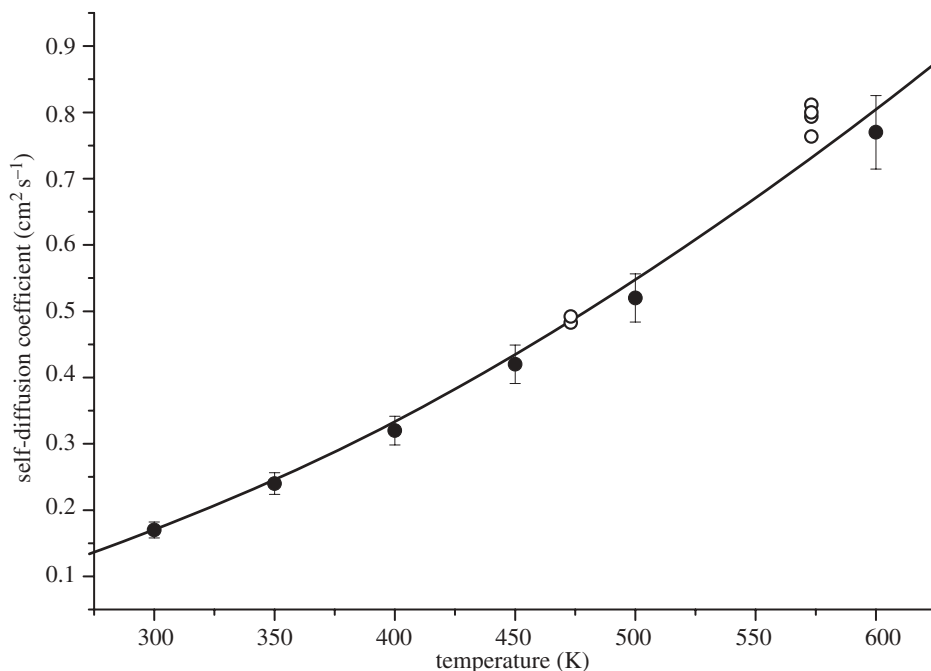


Figure 6. Self-diffusion coefficients of pure H<sub>2</sub>O (for 1 atm) versus temperature. Open circles and filled circles are measured values from Yoshida *et al.* [30] and Fokin & Kalashnikov [31], respectively, whereas the line gives direct results of molecular dynamics simulations with the intermolecular potential of Mas *et al.* [29].

with sh being the hyperbolic sine, which provides the quantities  $\Gamma_c(v)$  and  $\Delta_c(v)$  in equation (3.2).

- The velocity changes can be computed from classical molecular dynamics simulations (CMDS). The latter provide the time evolutions of the centre of mass positions and velocities (as well as molecular orientations and rotational angular momenta) of a large number of molecules starting from a pair-wise intermolecular potential. From these, the collision kernels can be directly deduced or modelled through an analytical law whose parameters are fitted to the proper velocity autocorrelation functions ([26,27] and references therein). Here, we use the Keilson & Storer (KS) [28] collision kernel (with the two parameters  $\nu_{VC}$  and  $\alpha$ ),

$$f_{KS}(v' \leftarrow v) = \nu_{VC} \times (1 - \alpha^2)^{-3/2} \times f_{MB} \left( \frac{v' - \alpha v}{\sqrt{1 - \alpha^2}} \right). \quad (3.5)$$

As in Tran *et al.* [26], we compute—from CMDS and the potential of Mas *et al.* [29]—the autocorrelation functions of the velocity  $\langle v(0) \times v(t) \rangle$  and energy  $\langle v(0)^2 \times v(t)^2 \rangle$ . Both functions decay exponentially, with time constants  $\tau_v$  and  $\tau_{v^2}$  related to the parameters  $\nu_{VC}$  and  $\alpha$  of equation (3.5), whose values for pure H<sub>2</sub>O at 296 K ( $\nu_{VC} = 0.053 \text{ cm}^{-1} \text{ atm}^{-1}$  and  $\alpha = 0.16$ ) were thus determined. Note that  $\tau_v$  is related to the mass diffusion coefficient,  $D = \tau_v k_B T / m$ , and the results in figure 6 demonstrate the quality of the present predictions, giving us confidence in our description of velocity changes.

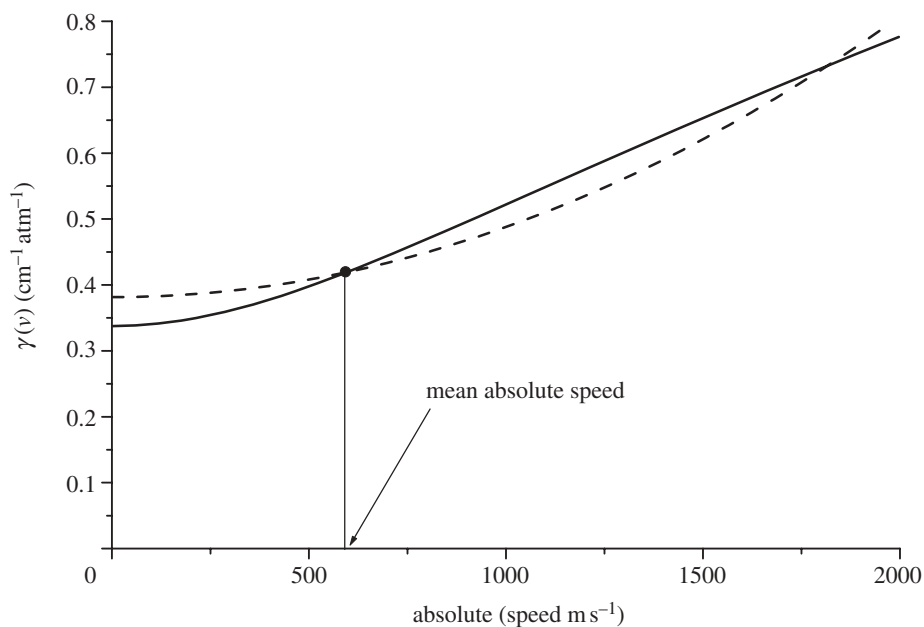


Figure 7. Speed dependence of the self-broadening of the  $6_{0,6} \leftarrow 5_{0,5}$  line of the  $2\nu_1 + \nu_2 + \nu_3$  band at room temperature. The solid line is values calculated with the semi-classical approach, whereas the dotted line is the quadratic law (slopes of  $\Gamma_0$  and  $\Gamma_2$  in figure 5) obtained from fits of measured spectra (figure 4) with a speed-dependent Voigt profile. Filled circles denote the experimental values of the mean broadening deduced from experiments (i.e. slope of  $\Gamma_0$  with SDV very close to that of  $\Gamma$  with the Rautian in figure 5).

It is interesting to compare the data calculated as explained earlier with those, displayed in figure 5, retrieved from the fits. For velocity changes, the slope of the Rautian profile narrowing parameter is about  $0.044 \text{ cm}^{-1} \text{ atm}^{-1}$ , close to CMDS predictions. The difference is likely due to the assumption of hard collisions (which correspond to  $\alpha = 0$  in the KS model) and to the neglect, by the Rautian profile, of the speed dependence (approximation compensated by the ad hoc value of  $\nu_{\text{VC}}$ ). Now considering the speed dependence of  $\Gamma$ , the CRB predictions can be compared with the quadratic law ( $\Gamma_0$  and  $\Gamma_2$  in figure 5) used in fits of figure 4. This is performed in figure 7 showing that these two approaches lead to a good agreement with the average broadening, but to different dependencies on the  $\text{H}_2\text{O}$  speed. Again, these differences are likely due to the fact that the SDVP fits neglect velocity changes, an approximation compensated through an ad hoc quadratic dependence.

Note that, in equation (3.2), velocity and internal state (rotation) changes appear as additive (uncorrelated) contributions that correspond to assuming that they occur in different collisions. In other words, a collision changes either the centre of mass velocity or the rotational angular momentum, but not both—a likely crude assumption. A simple correction was proposed by Rautian & Sobel'man [20], applied to  $\text{H}_2\text{O}$  spectra in Lisak *et al.* [14], which consists of replacing  $\nu_{\text{VC}}$  by  $\nu_{\text{VC}} - \eta(\Gamma_c - i\Delta_c)$ . We believe that CMDS can provide information on such correlations, and this possibility is currently under

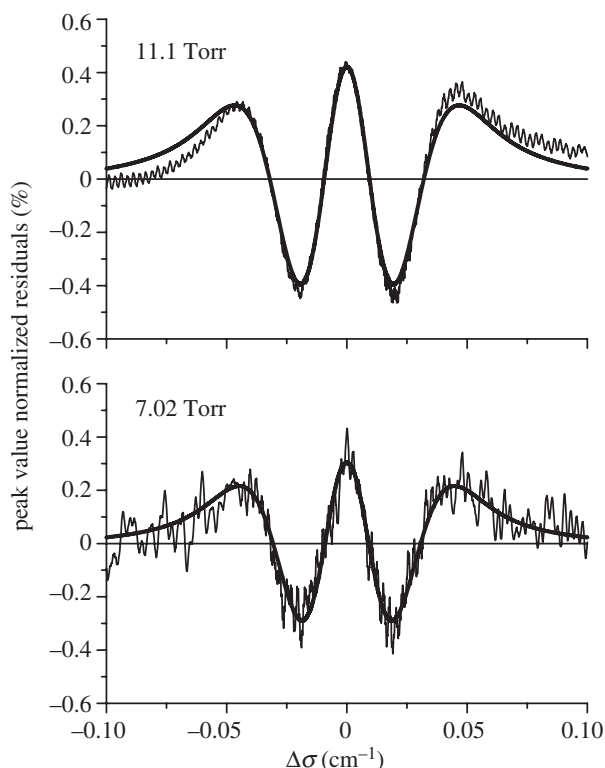


Figure 8. Residuals (normalized to the absorbance at the line peak) obtained from Voigt fits of measured (thin line) and calculated (thick line) spectra for the  $6_{0,6} \leftarrow 5_{0,5}$  line of the  $2\nu_1 + \nu_2 + \nu_3$  band of pure  $\text{H}_2\text{O}$  at room temperature and two pressures.

investigation. In the mean time, we decided to adjust  $\eta$  (about 0.3, independent of pressure for pure  $\text{H}_2\text{O}$  at room temperature) in order to ‘visually’ obtain a satisfactory agreement with the measurements in figure 4. Note that  $\eta$  is the only fitted parameter, all the others in equations (3.2)–(3.5) are fixed to CMDS and CRB predictions.

For comparisons of predictions with measurements, we use the procedure from Tran *et al.* [16]; i.e. for each pressure, we first compute the spectral shape using equations (3.1)–(3.3) and solve equation (3.2) numerically, as described by Tran & Hartmann [32]. Fitting this calculated spectrum using a Voigt shape provides the broadening coefficient and the fit residuals, two quantities that can be compared with those obtained from similar fits of the corresponding measured spectrum. This enables a meaningful test of the model that is much easier to implement than a least-squares fit of predictions to measured spectra. The results of this exercise, which need further investigation because they were obtained only a week before the ‘Water in the gas phase’ Theo Murphy meeting, are promising for two reasons. The first is that the broadening coefficients extracted from the Voigt fits of measured and calculated spectra agree within a couple of percent, a result expected from the quality of CRB calculations. The second is that figure 8 shows that fit residuals similar in magnitude and shape are obtained.

#### 4. Conclusion

This study indicates that the use of information from theoretical calculations based on the intermolecular potential is an interesting alternative to empirical approaches in order to model H<sub>2</sub>O line shapes beyond the Voigt profile. In fact, state-of-the-art semi-classical calculations provide a reliable description of the speed dependencies of the collisional-broadening and -shifting coefficients, whereas molecular dynamics simulations give information on the collision-induced changes of the velocity. Thus, all ingredients required for a description of speed-dependent, Dicke-narrowed line shapes can be obtained for modelling that are free of *a priori* assumptions and empirical parameters. Furthermore, such an approach enables a detailed analysis of the relative contributions of the various mechanisms. The results of this study—very preliminary since they were obtained just before the meeting—confirm previous ones [16], but require further investigation. These include studies for broad and narrow lines (low and high  $J$ ) of H<sub>2</sub>O with various perturbers (from very light to very heavy) at various temperatures and in a wide pressure range. Simultaneously, the correlation between velocity and rotational state changes due to collisions requires further investigation based on molecular dynamics simulations.

The authors from LISA thank the Institut du Développement et des Ressources en Informatique Scientifique (IDRIS) for giving access to the IBM Blue Gene/P parallel computer. J.M.H. thanks the Royal Society for providing support to the Theo Murphy meeting ‘Water in the gas phase’. R.R.G. acknowledges the support of this research by the National Science Foundation (grant no. ATM-0803135). Any opinions, findings and conclusions or recommendations expressed in this material are those of the author(s) and do not necessarily reflect the views of the National Science Foundation.

#### References

- 1 Gamache, R. R., Hartmann, J. M. & Rosenmann, L. 1994 Collisional broadening of water vapor lines—I. A survey of experimental results. *J. Quant. Spectrosc. Radiat. Transf.* **52**, 481–499. (doi:10.1016/0022-4073(94)90175-9)
- 2 Gamache, R. R. & Hartmann, J. M. 2004 An intercomparison of measured pressure-broadening and pressure shifting parameters of water vapor. *Can. J. Chem.* **82**, 1013–1027. (doi:10.1139/v04-069)
- 3 Anderson, P. W. 1949 Pressure broadening in the microwave and infra-red regions. *Phys. Rev.* **76**, 647–661. (doi:10.1103/PhysRev.76.647)
- 4 Tsao, C. J. & Curnutte, B. 1962 Line-widths of pressure-broadened spectral lines. *J. Quant. Spectrosc. Radiat. Transf.* **2**, 41–91. (doi:10.1016/0022-4073(62)90013-4)
- 5 Labani, B., Bonamy, J., Robert, D., Hartmann, J. M. & Taine, J. 1986 Collisional broadening of rotation–vibration lines for asymmetric-top molecules. I. Theoretical model for both distant and close collisions. *J. Chem. Phys.* **84**, 4256. (doi:10.1063/1.450047)
- 6 Labani, B., Bonamy, J., Robert, D. & Hartmann, J. M. 1987 Collisional broadening of rotation–vibration lines for asymmetric-top molecules. III. Self-broadening case: application to H<sub>2</sub>O. *J. Chem. Phys.* **87**, 2781–2789. (doi:10.1063/1.453065)
- 7 Lynch, R., Gamache, R. R. & Neshyba, S. P. 1996 Fully complex implementation of the Robert–Bonamy formalism: halfwidths and line shifts of H<sub>2</sub>O broadened by N<sub>2</sub>. *J. Chem. Phys.* **105**, 5711. (doi:10.1063/1.472416)

- 8 Ma, Q., Tipping, R. H. & Gamache, R. R. 2010 Uncertainties associated with theoretically calculated N<sub>2</sub>-broadened half-widths of H<sub>2</sub>O lines. *Mol. Phys.* **108**, 2225–2252. (doi:10.1080/00268976.2010.505209)
- 9 Gamache, R. R. & Hartmann, J. M. 2004 Collisional parameters of H<sub>2</sub>O lines: effects of vibration. *J. Quant. Spectrosc. Radiat. Transf.* **83**, 119–147. (doi:10.1016/S0022-4073(02)00296-0)
- 10 Wagner, G., Birk, M., Gamache, R. R. & Hartmann, J. M. 2005 Collisional parameters of H<sub>2</sub>O lines: effect of temperature. *J. Quant. Spectrosc. Radiat. Transf.* **92**, 211–230.
- 11 Antony, B. K. & Gamache, R. R. 2007 Self-broadened half-widths and self-induced line shifts for water vapor transitions in the 3.2–17.76 μm spectral region via complex Robert–Bonamy theory. *J. Mol. Spectrosc.* **243**, 113–123. (doi:10.1016/j.jms.2006.12.003)
- 12 Hartmann, J. M., Boulet, C. & Robert, D. 2008 *Collisional effects on molecular spectra. Laboratory experiments and model, consequences for applications*. Amsterdam, The Netherlands: Elsevier.
- 13 Brossmann, B. E. & Browell, E. V. 1989 Water-vapor line broadening and shifting by air, nitrogen, oxygen, and argon in the 720-nm wavelength region. *J. Mol. Spectrosc.* **138**, 562–595. (doi:10.1016/0022-2852(89)90019-2)
- 14 Lisak, D., Hodges, J. T. & Ciurylo, R. 2006 Comparison of semiclassical line-shape models to rovibrational H<sub>2</sub>O spectra measured by frequency-stabilized cavity ring-down spectroscopy. *Phys. Rev. A* **73**, 012507. (doi:10.1103/PhysRevA.73.012507)
- 15 De Vizia, M. D., Rohart, F., Castrillo, A., Fasci, E., Moretti, L. & Gianfrani, L. 2011 Speed-dependent effects in the near-infrared spectrum of self-colliding H<sub>2</sub>O<sup>18</sup> molecules. *Phys. Rev. A* **83**, 052506. (doi:10.1103/PhysRevA.83.052506)
- 16 Tran, H., Bermejo, D., Domenech, J. L., Joubert, P., Gamache, R. R. & Hartmann, J. M. 2007 Collisional parameters of H<sub>2</sub>O lines: velocity effects on the line-shape. *J. Quant. Spectrosc. Radiat. Transf.* **108**, 126–145. (doi:10.1016/j.jqsrt.2007.03.009)
- 17 Rothman, L. *et al.* 2008 The HITRAN 2008 molecular spectroscopic database. *J. Quant. Spectrosc. Radiat. Transf.* **110**, 533–572. (doi:10.1016/j.jqsrt.2009.02.013)
- 18 Hartmann, J. M., Taine, J., Bonamy, J., Labani, B. & Robert, D. 1987 Collisional broadening of rotation–vibration lines for asymmetric-top molecules. II. H<sub>2</sub>O diode laser measurements in the 400–900 K range; calculations in the 300–2000 K range. *J. Chem. Phys.* **86**, 144. (doi:10.1063/1.452605)
- 19 Rautian, S. G. & Shalagin, A. M. 1991 *Kinetic problems of non-linear spectroscopy*. New York, NY: Elsevier.
- 20 Rautian, S. G. & Sobel'man, J. I. 1967 The effect of collisions on the Doppler broadening of spectral lines. *Sov. Phys. Usp.* **9**, 701. (doi:10.1070/PU1967v009n05ABEH003212)
- 21 Galatry, I. 1961 Simultaneous effect of Doppler and foreign gas broadening on spectral lines. *Phys. Rev.* **122**, 1218–1223. (doi:10.1103/PhysRev.122.1218)
- 22 Nelkin, M. & Ghatak, A. 1964 Simple binary collision model for Van Hove's  $G_s(r, t)$ . *Phys. Rev.* **135**, A4–A9. (doi:10.1103/PhysRev.135.A4)
- 23 Ngo, N. H. *et al.* In press. Line intensity and line-shape of H<sub>2</sub>O in the near-infrared by tunable diode laser spectroscopy. *J. Quant. Spectrosc. Radiat. Transf.* (doi:10.1016/j.jqsrt.2011.12.007)
- 24 Ibrahim, N., Chelin, P., Orphal, J. & Baranov, Y. I. 2008 Line parameters of H<sub>2</sub>O around 0.8 μm studied by tuneable diode laser spectroscopy. *J. Quant. Spectrosc. Radiat. Transf.* **109**, 2523–2536. (doi:10.1016/j.jqsrt.2008.04.008)
- 25 Rohart, F., Włodarczyk, G., Colmont, J. M., Cazzoli, G., Dore, L. & Puzzarini, C. 2008 Galatry versus speed-dependent Voigt profiles for millimeter lines of O<sub>3</sub> in collision with N<sub>2</sub> and O<sub>2</sub>. *J. Mol. Spectrosc.* **251**, 282–292. (doi:10.1016/j.jms.2008.03.005)
- 26 Tran, H., Hartmann, J. M., Chaussard, F. & Gupta, M. 2009 An isolated line-shape model based on the Keilson and Storer function for velocity changes. II. Molecular dynamics simulations and the Q(1) lines for pure H<sub>2</sub>. *J. Chem. Phys.* **131**, 154303. (doi:10.1063/1.3247898)
- 27 Tran, H., Thibault, F. & Hartmann, J. M. 2011 Collision induced velocity changes from molecular dynamic simulations: application to the spectral shape of the Q(1) Raman transition of H<sub>2</sub> perturbed by Ar. *J. Quant. Spectrosc. Radiat. Transf.* **112**, 1035–1042. (doi:10.1016/j.jqsrt.2010.12.004)

- 28 Keilson, J. & Storer, J. E. 1952 On Brownian motion, Boltzmann's equation, and the Fokker–Planck equation. *Q. Appl. Math.* **10**, 243–253.
- 29 Mas, E. M., Bukowski, R., Szalewicz, K., Groenenboom, G. C., Wormer, P. E. S. & van der Avoird, A. 2000 Water pair potential of near spectroscopic accuracy: I. Analysis of potential surface and virial coefficients. *J. Chem. Phys.* **113**, 6687. (doi:10.1063/1.1311289)
- 30 Yoshida, K., Matubayasi, N. & Nakahara, M. 2006 Self-diffusion of supercritical water in extremely low-density region. *J. Chem. Phys.* **125**, 074307 (doi:10.1063/1.2333511)
- 31 Fokin, L. R. & Kalashnikov, A. N. 2008 The viscosity and self-diffusion of rarefied steam: refinement of reference data. *High Temp.* **46**, 614–619. (doi:10.1134/S0018151X08050040)
- 32 Tran, H. & Hartmann, J. M. 2009 An isolated line-shape model based on the Keilson and Storer function for velocity changes. I. Theoretical approaches. *J. Chem. Phys.* **130**, 094301. (doi:10.1063/1.3073758)